ELSEVIER

Journal of Chromatography A, 838 (1999) 71–80

JOURNAL OF CHROMATOGRAPHY A

Isotachophoretic focusing of strong and weak electrolytes in combined pH and conductivity gradients

Tomáš Rejtar, Karel Šlais*

Institute of Analytical Chemistry, Academy of Sciences of the Czech Republic, Veveří 97, 611 42 Brno, Czech Republic

Abstract

Isotachophoretic focusing of weak and strong electrolytes on the background with combined pH and conductivity gradients generated by the stacking of synthetic polyampholytes was studied. The simple theoretical model for the calculation of the position and separation of analyte zones was suggested. The model was experimentally verified by focusing of derivatized poly(ethylene glycols), poly(tetrahydrofurans) and nitrophenols. The influence of pH of the leading electrolyte and the effective charge of analyte on the separation of derivatives of weak acids with different pK_a values and ionic mobilities was examined.

Keywords: Isotachophoresis; pH gradients; Conductivity gradients; Buffer composition; Stacking; Nitrophenols; Phenols; Poly(ethylene glycol); Poly(tetrahydrofuran); Benzoic acids

1. Introduction

Isotachophoretic focusing (ITF) is an electromigration analytical method with a unique possibility to focus and separate into the Gaussian shaped zones several kinds of electrolytes including weak, strong and amphoteric ones. This method was introduced as isotachophoresis (ITP, [1,2]) with carrier ampholytes [3–7]. A similar electrophoretic mode also occurs for the mobilization of focused analytes in isoelectric focusing (IEF) known as isoelectric focusing with electrophoretic mobilization [8–12]. ITF was used mainly for separation of proteins [1,13–15].

The design of the experiment is similar to that of ITP and can be done in the following way, see Fig. 1. The sample and the carrier ampholytes are injected between the leading (LE) and terminating electrolytes (TE). When the electric current is switched on, all charged compounds start to move in one direction. After sufficient time, the system reaches the steady state; then the carrier ampholytes and analytes are ordered according to their effective mobilities according to the isotachophoretic rules, see Fig. 1a and 1b. Further, the continual conductivity gradient [3,4] is formed from the great number of individual ampholytes with different effective mobilities present in the carrier ampholytes [16,17], Fig. 1c. The pH gradient is established simultaneously according to the differences in pH of ordered zones of ampholytes [8–11,18], Fig. 1c. As a result of the equilibrium between the self sharpening effect and the diffusion and since the maximum concentrations of the zones of analytes are too low to form square shaped zones typical for ITP, the analytes form Gaussian shape zones similar to IEF, Fig. 1b. In other words, the ionic analytes are separated and focused on the background of the

*Corresponding author. Tel.: +42-5-7268-211, Fax: +42-5-4121-2113.

E-mail address: slais@iach.cz (K. Šlais)

0021-9673/99/$ – see front matter
PII: S0021-9673(98)01003-6

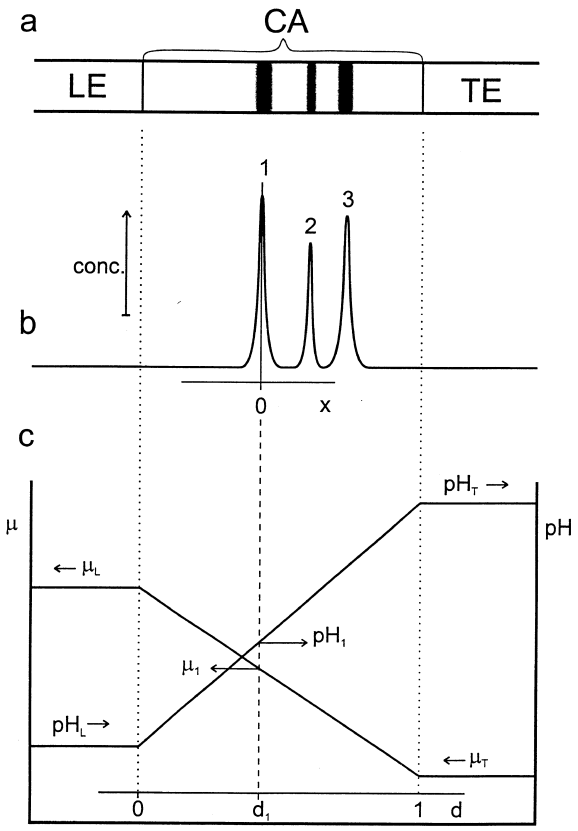

Fig. 1. Illustration of the separation principle of IEF. (a) Schema of the electrolytes in the steady state; (b) concentration profiles of focused analytes marked 1, 2 and 3; (c) scheme of the course of the mobility and pH gradients. The pH_1, μ_1 and d_1 are properties of the analyte No. 1 zone. X is an axis in coordinate system moving together with the peak of analyte so that the zero of the coordinate system is always at the peak maximum. LE = Leading electrolyte, TE = terminating electrolyte, CA = carrier ampholytes, symbols with indexes L and T are related to leading and terminating electrolytes, respectively.

continual pH and conductivity gradients generated by the carriers.

In most of the references [1,3,19,20], an approximately linear pH gradient was considered and the separation mechanism was supposed to be similar to that of IEF. Nevertheless, as stated above, the conductivity gradient occurs in the isotachophoretically moving stack of carrier ampholytes [1,3,4,21]. This was proven by separation of strong electrolytes which should not be influenced by pH gradient [3,4]. Charlionet and co-workers [21,22] tried to suggest a model of separation of electrolytes in mobility gradient without considering the pH gradient. The model of behaviour of strong and weak electrolytes in a combined pH and conductivity gradient was suggested [23] and experimentally verified for strong electrolytes recently [24].

In the present contribution, the previous model [23] was modified and applied to the focusing and separation of both weak and strong electrolytes in a combined pH and conductivity gradient. Further, under the assumption of linearity of both mobility and pH gradients, the positions of strong and weak electrolytes in the gradients were calculated. The model was experimentally verified by focusing of derivatized poly(ethylene glycols) (PEGs), poly-(tetrahydrofurans) and nitrophenols on the background of synthetic polyampholytes. The influence of pH of the leading electrolyte on the separation of derivatives of weak acids with different pK values and ionic mobilities was examined.

2. Theory

As stated in Section 1, the design of ITF is formally very similar to that of ITP. Firstly, let us consider only the injection of carrier ampholytes without the sample. The separation of zones of carriers leads to the generation of two gradients: mobility and pH gradients. The span of the pH and mobility is in the range of the mobilities and pH values of LE and TE, respectively. However, the pH and mobility of TE are governed both by composition of TE and by the composition of the LE and that is why it is not possible to change the span of pH and conductivity gradients independently. Due to the ITP migration of whole stack, the ampholytes are focused out of their isoelectric point (pI) and respective deviations are inversely proportional to their steepness of titration curve close to their pI, $(dz/dpH)_{pI}$, see, e.g., Refs. [19,25].

The gradient of mobility in the isotachophoretically moving stack of carrier ampholytes can be expressed in terms of conductivity. Under the steady state, we can write

$$\mu = \frac{\nu\kappa A}{I} \tag{1}$$

where ν is isotachophoretic velocity, κ is conduc-

tivity, A is a cross section and I is electric current. Since the ν, A and I terms are constant, the conductivity of the background at particular position in the gradient is linearly related to the effective mobility of components focused at the respective place. Thus, mobility and conductivity gradients of the background are parallel, but the term ''gradient of conductivity'' better expresses the physical variable of the background which is responsible for the focusing of analytes. Further, the conductivity can be written as resistivity $\rho = 1/\kappa$ as used previously [23,24].

To show the basic role of the combined conductivity and pH gradient in ITF and to simplify the calculations, let us assume the linearity of mobility and pH gradients between LE and TE, see Fig. 1c. Then, it is possible to express the gradients as functions of position in the carrier ampholyte stack, d

$$\mathrm{pH}_d = (\mathrm{pH_T} - \mathrm{pH_L})d + \mathrm{pH_L} \tag{2}$$

$$\mu_d = (|\mu_\mathrm{T}| - |\mu_\mathrm{L}|)d + |\mu_\mathrm{L}| \tag{3}$$

Here, d is dimensionless distance between the LE and TE. For the boundary between the LE and stack of ampholytes, LE/CA, it is $d = 0$ and for the boundary between stack of ampholytes and the TE, CA/TE, it is $d = 1$. When the stack moves with constant velocity then we can derive the time of detection, t_{det}, of position d as follows

$$t_{\mathrm{det}} = \frac{dL_\mathrm{g}}{\nu} + k \tag{4}$$

where k is a system constant and L_g is the length of the gradients.

Now, let us assume that the analyte consists of weak electrolyte, i, with its $\mathrm{p}K_{\mathrm{a},i}$ and $\mu_{0,i}$ values within the range of the mobilities and pH values set by LE and TE and that the concentration of the analyte is so low in comparison with concentration of carrier ampholytes forming the background that the presence of sample cannot influence the shape of the gradients. Under steady state, when the analyte velocity reaches the isotachophoretic velocity of the stack, the analyte is focused at such a place of the combined gradient, where pH of analyte zone pH_i equals local pH of the gradient, $\mathrm{pH}_i = \mathrm{pH}_d$, and effective mobility of analyte zone equals local effective mobility of the stack, $\mu_i = \mu_d$. This relations follow directly from the assumption of low concentrations of analyte in comparison with the background concentration.

It holds for the weak electrolyte with effective mobility, μ_i

$$\mu_i = \mu_{0,i}\frac{K_{\mathrm{a},i}}{K_{\mathrm{a},i} + [\mathrm{H}^+]} \tag{5}$$

According to the above assumption of linear gradients described by Eqs. (2) and (3) we can write implicit function for the position of the analyte peak as

$$(|\mu_\mathrm{T}| - |\mu_\mathrm{L}|)d + |\mu_\mathrm{L}| = \mu_{0,i}\frac{K_{\mathrm{a},i}}{K_{\mathrm{a},i} + 10^{-[(\mathrm{pH_T} - \mathrm{pH_L})d + \mathrm{pH_L}]}} \tag{6}$$

This equation can be solved and the position of the analyte can be calculated. Further, it is possible to calculated analyte effective mobility, pH and the degree of dissociation.

Peak variance of the focused peak can be expressed according to Ref. [23] as follows

$$\sigma^2 = -\frac{D}{\mathrm{d}\nu/\mathrm{d}x} \tag{7}$$

where D is a analyte diffusion coefficient and $\mathrm{d}\nu/\mathrm{d}x$ is the gradient of the migration velocity along the analyte zone, x is the length coordinate along the moving carrier ampholytes stack with $x = 0$ at the peak maximum, see Fig. 1b.

3. Experimental

3.1. Equipment

An automated miniaturized instrument, which has been described previously [19,20,25], was used throughout the separations. It consists of liquid handling device controlled by microprocessor and a separation compartment. To reduce the overall applied voltage for the separation, the taper shaped capillary channel was used [19,20,25–27]. The overall volume of the separation compartment is approxi-

mately 9.5 μl. The inlet diameter of the tapered plastic channel is 0.8 mm and it decreases to 0.4 mm then follows a 5-cm long fused-silica capillary with inner diameter 0.32 mm and then follows a 5-cm long fused-silica capillary 0.25 mm I.D. with detection window. A UV–Vis detector LCD 2082 (Ecom, Prague, Czech Republic) was connected by 0.2-mm optical fibers [28] to the detection window. The analytical signal was collected by a personal computer equipped with data handling software (DataApex, Prague, Czech Republic). A high-power supplier from Spellman CZE 1000R (New York, USA) was used.

3.2. Chemicals

All chemical were analytical grade. PEG $M_r = 200$ g mol^{-1}, poly(tetrahydrofuran) $M_r = 250$ g mol^{-1}, 4-hydroxy-3-nitrobenzoic acid, 3-chloro-4-hydroxybenzoic acid hemihydrate, 2-nitrophenol (2-NP) and 3-nitrophenol (3-NP) were obtained from Aldrich (Milwaukee, WI, USA); tris(hydroxymethyl)aminomethane (Tris), 2-sulfobenzoic acid cyclic anhydride, sodium hydroxide and sulfuric acid from Lachema (Brno, Czech Republic), 2-hydroxyisobutyric acid (HIBA) from Fluka (Buchs, Switzerland), 2-(cyclohexylamino) ethanesulfonic acid (CHES) from Merck (Darmstadt, Germany), 4-methyl-2-nitrophenol and hydroxypropylmethyl cellulose (HPMC) from Sigma (St. Louis, MO, USA) and polyethylenimine (PEI) from Serva (Heidelberg, Germany) The solution of synthetic carrier ampholytes pH 3.5–10 was purchased from Pharmacia (Uppsala, Sweden).

3.3. Electrolyte system

A solution of 10 m*M* HIBA (leader) and Tris buffer was used as a leading electrolyte for all of the analysis. The pH of the leading electrolyte (pH_L) was varied in two ranges. The first one was from 6.6 to 9.0 where the $Tris/Tris^+$ served as buffering system and the second one was around pH = 4.7 where $HIBA/HIBA^-$ behaved as a buffering system. A mixture of 50 m*M* CHES and 5 m*M* NaOH was used as the terminating electrolyte. All of the experiments were carried out in the closed mode of ITP and which is why the control of endoosmotic flow was necessary. The dynamic coating [29–31] of the separation compartment by adding 0.06% (w/v) HPMC and 2.5 μg ml^{-1} PEI [32] was chosen. The pH_L was measured before PEI was added into the leading electrolyte to avoid the contamination of the pH electrode by surface active compound. A solution of 4% (v/v) ampholine served as carrier ampholyte.

3.4. Preparation of model analytes

For preparation of model strong analytes the esterification reaction [24] was used. 1.0 g of polyethylene glycol 200 was mixed with 0.1 g of 2-sulfobenzoic acid cyclic anhydride and heated for 7 h at 100°C. Similarly, the derivatized poly(tetrahydrofurans) were prepared. For preparation of weak electrolyte model analytes the following procedure was used. Twenty mg of 4-hydroxy-3-nitrobenzoic acid (or 3-chloro-4-hydroxybenzoic acid hemihydrate) was mixed with 1.0 ml poly(tetrahydrofuran) and with one droplet of concentrated sulfuric acid. This mixture was then heated for 20 min at 120°C. For analysis approximately hundred-fold diluted solutions were injected.

The values of pK_a and ionic mobilities of analytes used for calculations of their zone positions in combined pH and mobility gradients are summarized in Table 1.

4. Results and discussion

4.1. Separation and focusing of model mixtures in combined pH and mobility gradients

The analysis of homologous series of esters of strong and weak acids in the combined pH and conductivity gradients were performed. As indicated in Section 2, the separation is influenced by the parameters of gradients such as pH and conductivity ranges and the slopes of the gradients. This influence was demonstrated by the change in the composition of the LE. The change in the pH of the LE was accomplished by varying in the concentration of the counterion in the LE although the buffer capacity of such system is changed. Considering very low concentration of the sample in comparison with the background, the pH of LE can be varied in the range

Table 1
Properties of compounds used for the calculation

Compound	pK_a	|Mobility| (10^{-9} V m^2 s^{-1})
2-Nitrophenol	7.23[a]	33.4[a]
3-Nitrophenol	8.40[a]	33.4[a]
4-Methyl-2-nitrophenol	7.47[b]	32.4[c]
First[f] member of series of polytetrahydrofuran esters of		
4-hydroxy-3-nitrobenzoic acid	5.7[d]	25.6[e]
3-chloro-4-hydroxybenzoic acid	7.0[d]	26.4[e]
2-sulfobenzoic acid	–	24.2[e]
HIBA	3.97[a]	33.5[a]
Tris	8.07[a]	26.9[a]
CHES	9.3	22

[a] From Ref. [33].
[b] From Ref. [34].
[c] Estimation from the values of similar compounds (phenol, 4-methylphenol and 2-nitrophenol).
[d] Determined by potentiometric titration.
[e] Estimated from equation mobility = $1515M_r^{-0.7372}$ derived for PEGs according to Ref. [24].
[f] Values of pK_a for second, third and forth members are assumed to be the same as for monomers. The mobility of second, third and forth members were calculated according to footnote e.

p$K_a \pm 1 \div 2$ in this way. The impact of pH of LE on parameters of the gradients was estimated by Becker's procedure [35]. The results of the calculations are summarized in Table 2. Further explanation is made in the following paragraph.

The examples of the analysis of homologous series of esters of weak and strong acids for two pH values of LE are presented in Fig. 2. In Fig. 2a (i) and Fig. 2b (i), the parallel analysis of similar derivates of strong acid with known ionic mobilities is presented. Since these compounds are not influenced by pH

Table 2
Parameters of the separation window for system LE: 10 m*M* HIBA, titrated by Tris buffer to pH_L, TE: adjusted zones of CHES

pH_L	pH_T	$-\mu_L$ (10^{-9} V m^2 s^{-1})	$-\mu_T$ (10^{-9} V m^2 s^{-1})
4.75	8.63	28.7	3.9
6.00	8.69	33.2	4.4
6.50	8.70	33.4	4.4
7.00	8.72	33.5	4.6
7.50	8.77	33.5	5.0
8.00	8.89	33.5	6.1
8.50	9.09	33.5	8.4
9.00	9.38	33.5	12.0

For more details see text.

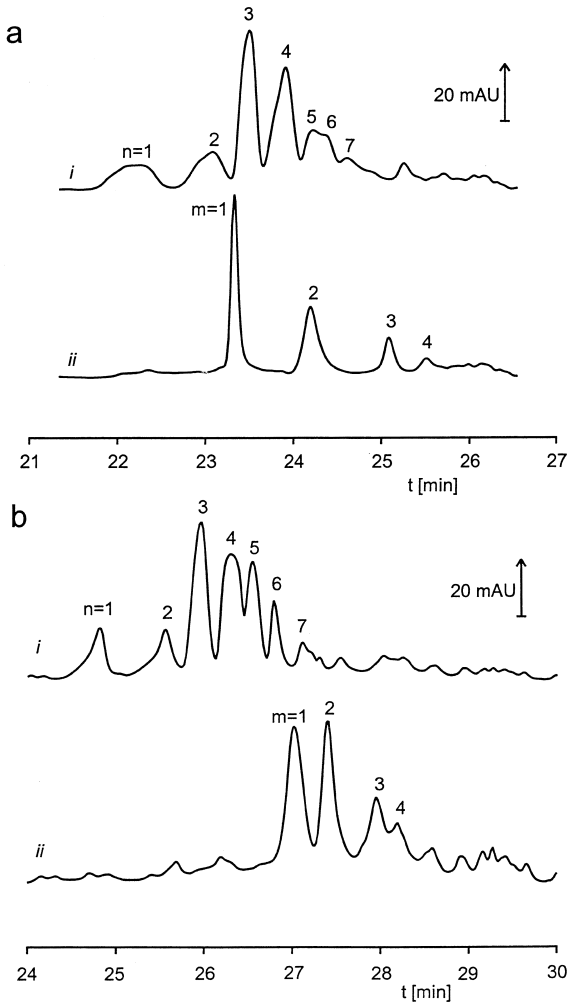

Fig. 2. Analysis of derivatized polymers with different pH of LE in (a) pH = 8.50 and in (b) pH = 6.92. Other conditions: LE: 10 m*M* HIBA and appropriate amount of Tris, 0.06% HPMC, 2.5 μg/ml PEI; TE: 50 m*M* CHES, 5 m*M* NaOH; background 4% ampholine pH 3.5–10.0; sample volume 500 nl, background volume 400 nl; current = 15 μA, λ = 270 nm. *n* indicates the number of monomers in poly(ethylene glycol) esters of 2-sulfobenzoic acid (records i) and *m* indicates the number of monomers in poly(tetrahydrofuran) esters of 4-hydroxy-3-nitrobenzoic acid (records ii).

gradient and the separation is achieved only by the conductivity gradient, the difference in the records in Fig. 2a (i) and Fig. 2b (i) is only due to the differences in the conductivity gradients. It is apparent that the records of weak acid derivatives with LE of lower pH, Fig. 2b (ii), are delayed in comparison

with the same analyte in analysis of LE with higher pH, Fig. 2a (ii). Thus, pH of the LE has larger effect on weak acid analytes than strong ones, which will be discussed in terms of theory described in Sections 4.2 and 4.3. The unsymmetrical profile of the peaks of analytes can probably be explained by non-linearities of the gradients and will be discussed later in Section 4.4.

4.2. Dependence of analyte effective mobility on pH_L

The changes of mobilities in model analytes are visualized by the changes in their migration times as presented in Fig. 2. When the profile of the gradients can be considered as reproducible [24] we can assign migration times in the gradient to their corresponding effective mobilities as follows from ITP rules. The dependence of mobility vs. migration time was approximated by the parallel analysis of the mixture of strong anions with known mobilities. As standards served the model mixture of PEGs derivatized by 2-sulfobenzoic acid, which are strong electrolytes which is why their migration times are not influenced by pH gradient [24]. This mixture was analyzed for each pH of LE and the dependence of mobilities vs. migration times were approximated by linear regression. The squares of regression coefficients were always higher then 0.996 for all dependencies. Because of the lack of low mobility standards ($|\mu| < 15 \cdot 10^{-9}$ m^2 V^{-1} s^{-1}) it was necessary to expand the linear regression down to $|\mu| \approx 5 \cdot 10^{-9}$ m^2 V^{-1} s^{-1}, which corresponds to the lowest studied analyte mobility. The obtained dependence of effective mobility vs. pH of LE is presented in Fig. 3a. As expected, we can see no dependence on pH of LEs for strong electrolytes, see Fig. 3a, curve 1. For various weak electrolytes, see curves 2–6 obtained as fits to the respective experimental points, their effective mobilities under steady state strongly depend on pH of the LE and thus on the parameters of the gradients. Curves 3 and 2 correspond to 1,4-butanediol esters of chloro- and nitro-hydroxybenzoic acid, respectively and curves 4, 5 and 6 correspond to three nitrophenols. The ionic mobilities and pK_a values of these weak anions are summarized in Table 1.

In Fig. 3b, the dependencies calculated according

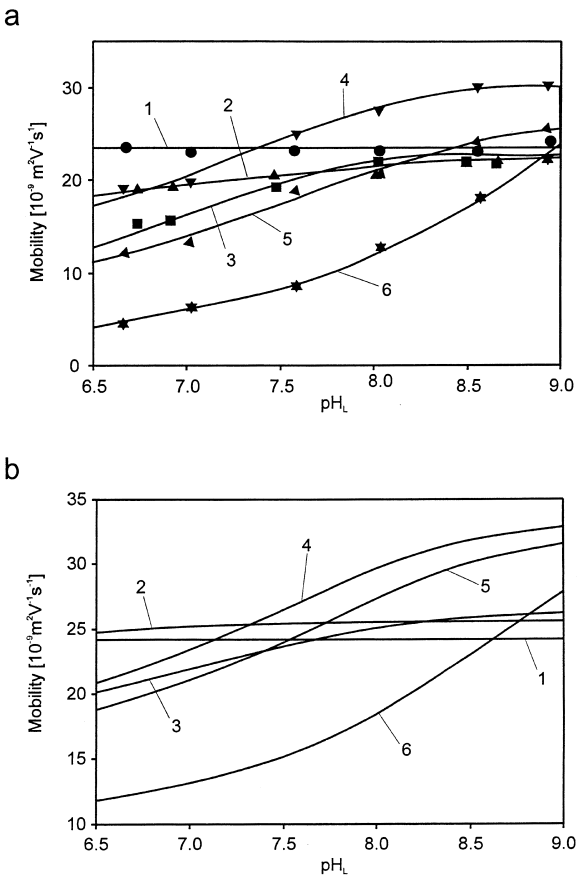

Fig. 3. Dependence of analyte effective mobility on pH of leading electrolyte. (a) Experimental values, (b) values calculated on the assumption of linearity of mobility and pH gradients. The parameters of the gradients are shown in Table 2. Analytes: 1=mono(ethylene glycol) ester of 2-sulfobenzoic acid, 3=mono(tetrahydrofuran) ester of 3-chloro-4-hydroxybenzoic acid, 2=mono(tetrahydrofuran) ester of 4-hydroxy-3-nitrobenzoic acid, 4=2-nitrophenol, 5=4-methyl-2-nitrophenol, 6=3-nitrophenol.

to the model with the assumption of linear course of both conductivity and pH gradients, see Section 2, are shown. For the calculation of this dependencies, the analyte ionic mobility and pK_a and also the parameters of the gradients must be known. The values of ionic mobilities and pK_a were taken from Table 1. For the calculation of parameters of linear gradients we have to know at least two points in each gradient. The mobility and pH corresponding to one point was calculated from the composition of leading electrolyte. For the second point, the mobility and pH of the TE (in all cases CHES) was used. These

values were calculated by Becker's procedure [35]; results are in Table 2. Although the values of mobilities in Fig. 3b do not exactly agree to the experimental values in Fig. 3a, the courses of the corresponding curves are very similar. Indeed, the shapes of curves in Fig. 3 can be characterized as a part of sigmoidal dependence according to Eq. (5). The differences can be caused by inaccuracy of pK_a values and ionic mobilities of the analytes and, of course, mainly by the simplification of the theory and the poor estimation of the parameters of the gradients. However, we can consider that the above described model is in qualitative agreement with experimental observations.

Since the analyte effective mobility under steady state is related to the peak position in the gradient generated by the stack, the curves in Fig. 3 illustrate how the distance between the zones of analytes and the selectivity can be controlled by choice of leading electrolyte pH.

4.3. Calculation of the position of analytes in the gradient, dependence of selectivity on the parameters of analytes

In above sections, it was demonstrated both on the suggested model and experimentally, that the position of analyte in the gradient is dependent both on the parameters of gradient and of analyte. Here, the use of suggested model to predict the selectivity of separation is shown. In Fig. 4a, the combined linear pH and linear mobility gradient determined by mobility window from -3.9 to $-28.7\cdot10^{-9}$ m^2 V^{-1} s^{-1} and pH window from 4.8 to 8.5 is shown, the values are summarized in Table 2.

Using the model described in Section 2, Eq. (6) and ionic mobilities from Table 1, the positions of series of weak analytes with p$K_a=7.0$ (Fig. 4b, i) and 5.7 (Fig. 4b, ii) as well as strong analytes (Fig. 4b, iii) were calculated. As expected, the analytes with higher pK_a are shifted toward the basic end of the stack. What is not so easy to foresee, the compounds with the similar differences in the ionic mobilities should be focused closer each other when their pK_a is higher. The calculated positions are summarized in more detail, in Table 3. The predicted dependence of analyte peak position on analyte pK_a was verified by ITF of a series of derivatized poly(tetrahydrofurans), see Fig. 4c, i–iii. It can be seen that the predicted increase in the selectivity with decrease in the analyte pK_a values is well documented. The practical issue of this finding is that the gradient and/or derivatizing reagent should be chosen so that the dissociation degree of analyte should be the highest possible. In that way the selectivity in the separation of homological series will be high.

4.4. Course of local gradients – gradient waving

In Ref. [24] it was stated that the local steepness of the gradients in carrier ampholytes strongly influences not only the position of the analyte zone but also the shape and width of the analyte zone. For visualization of this ''gradient waving'', the properties of carrier ampholytes can be employed. It is well known that the carrier ampholytes well absorb at wavelengths bellow 250 nm and the absorbance is apparently different for each particular component [16,17,36]. The optical profile of the focused stack obtained by monitoring of the absorbance at 230 nm and injecting the water as the sample is presented in Fig. 5(i). The record in Fig. 5 (ii) is analysis under the same conditions the but monitored at 270 nm and with derivatized PEGs as the sample. Fig. 5 (ii) shows that the peak widths of analytes are different at different parts of the focused stack. When comparing these widths with those at corresponding places in the stack of carrier ampholytes we can see similar trends in peak widths of both the carrier ampholytes and analytes. When zones at particular place of the carrier ampholytes stack are narrower, the analyte peaks at corresponding place are narrower, too. So it is possible to conclude that the analyte peak width is dependent on the separation pattern of carrier ampholytes.

5. Conclusions

It was shown that the separation of weak and strong electrolytes in combined pH and conductivity gradients is in qualitative agreement with the theory described in Ref. [23]. Further, the enhancement of

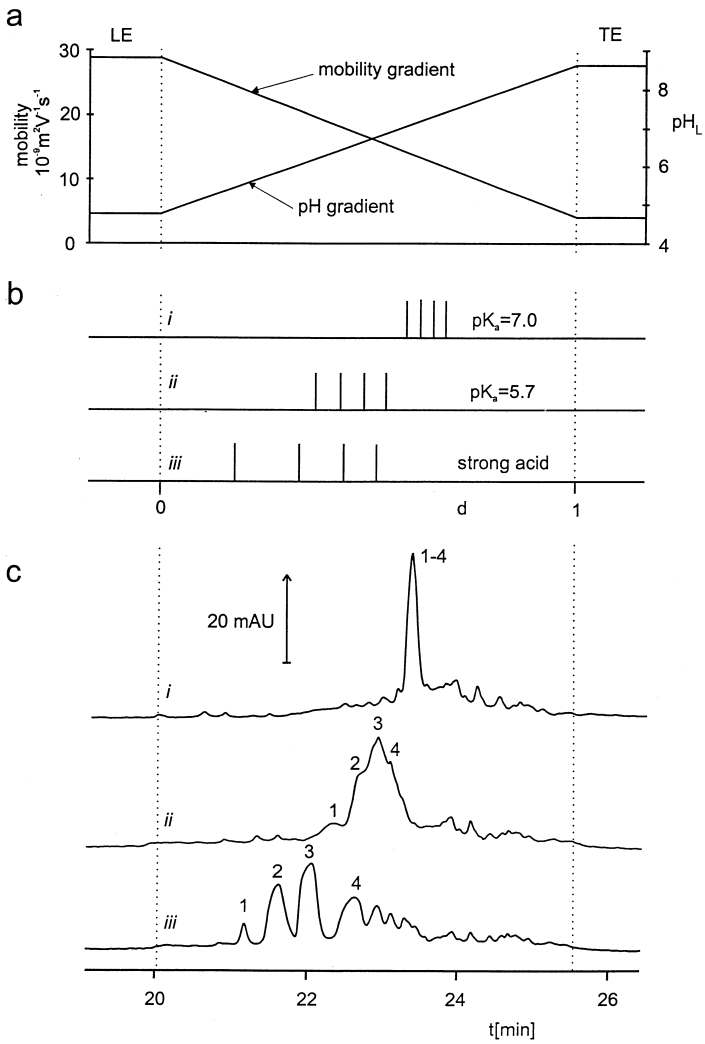

Fig. 4. Comparison of calculated positions of weak electrolytes in gradients with the experimental values. (a) Design of the model; (b) calculated position of the analytes; (c) experimental position of analytes. pH of leading electrolyte = 4.75; other conditions as in Fig. 2. Records indicated as i, ii, iii correspond to analytes 3, 2 and 1, respectively, in Fig. 3.

this theory for the calculation of position of analyte zones in the carrier ampholyte stack was made under the assumption of linear pH and mobility gradient. The calculated and found positions of the analyte zones were in a good agreement and that is why it is well-founded to approximate the gradients with linear function. However, it was shown that the gradients have only linear trend but they are waved. It was found that high effective charge of analyte is optimal for achieving high selectivity of separation in ITF. Since the high effective charge of analyte was found previously [37] to be advantageous for obtaining of the narrow peaks in CZE, it should be important also for gain in resolution in ITF. In the future, the possibility of preparation of more homogeneous background with possibility to inde-

Table 3
Theoretical and experimental positions of analyte zones in combined mobility and pH gradients

Derivative of	No. of monomer units of oligo tetrahydrofurans	*d*	
		Theoretical	Experimental
2-Sulfobenzoic acid	1	0.180	0.209
	2	0.335	0.291
	3	0.442	0.368
	4	0.521	0.471
4-Hydroxy-3-nitrobenzoic acid	1	0.374	0.325
	2	0.424	0.482
	3	0.491	0.529
	4	0.545	0.573
3-Chloro-4-hydroxybenzoic acid	1	0.593	0.582
	2	0.627	–
	3	0.656	–
	4	0.682	0.645

pendently set up the pH and conductivity gradients will be studied.

Acknowledgements

This work was supported by grant of the Academy of Sciences of the Czech Republic, No. A 4031504.

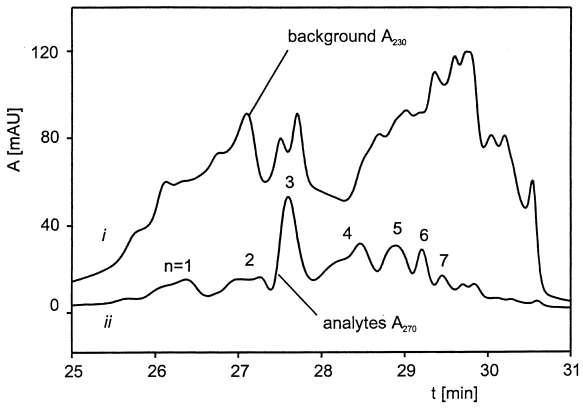

Fig. 5. Illustration of gradient waving. *n* indicates the number of monomer unites in poly(ethylene glycol) esters of 2-sulfobenzoic acid. Further explanation in Section 4.4.

References

[1] F.M. Everaerts, J.L. Beckers, Th.P.E.M. Verheggen, Isotachophoresis, Elsevier, Amsterdam, 1976.
[2] P. Boček, M. Deml, P. Gebauer, V. Dolník, Analytical Isotachophoresis, VCH, Weinheim, 1988.
[3] T. Manabe, H. Yamamoto, T. Okuyama, Electrophoresis 10 (1989) 172.
[4] H. Yamamoto, T. Manabe, T. Okuyama, J. Chromatogr. 480 (1989) 331.
[5] P. Delmotte, Sci. Tools 24 (1977) 33.
[6] F.M. Everaerts, M. Guerts, F.E.P. Mikkers, Th.P.E.M. Verheggen, J. Chromatogr. 119 (1976) 129.
[7] F. Acevedo, J. Chromatogr. 470 (1989) 407.
[8] S. Hjertén, M. Zhu, J. Chromatogr. 387 (1987) 127.
[9] J. Čáslavská, S. Molteni, J. Chmelík, K. Šlais, F. Matulík, J. Chromatogr. A 680 (1994) 549.
[10] J.R. Mazzeo, I.S. Krull, Anal. Chem. 63 (1991) 2852.
[11] F. Kilár, S. Hjertén, Electrophorersis 10 (1989) 23.
[12] T. Izumi, T. Nagahori, T. Okuyama, J. High Resolut. Chromatogr. 14 (1991) 351.
[13] F. Acevedo, J. Chromatogr. 545 (1991) 391.
[14] P. Delmote, in: Electrophoresis '78, Elsevier/North Holland, 1978, p. 115.
[15] S. Hjertén, M. Kiessling-Johansson, J. Chromatogr. 550 (1991) 811.
[16] P.G. Righetti, J. Chromatogr. 190 (1980) 275.
[17] O. Vesterberg, Ann. NY Acad. Sci. 209 (1973) 23.
[18] K. Šlais, J. Microcol. Sep. 5 (1993) 469.
[19] M. Št'astná, Ph.D. Thesis, Brno, 1996.
[20] M. Št'astná, V. Kahle, K. Šlais, J. Chromatogr. A 730 (1996) 261.

[21] R. Charlionet, A. Bringard, Ch. Davrinche, M. Fontaine, Electrophoresis 7 (1986) 558.
[22] A. Bringard, R. Charlionet, Electrophoresis 11 (1990) 802.
[23] K. Šlais, J. Chromatogr. A 764 (1997) 309.
[24] T. Rejtar, K. Šlais, J. Chromatogr. A 798 (1998) 223.
[25] M. Št'astná, K. Šlais, J. Chromatogr. A 768 (1997) 283.
[26] K. Šlais, J. Chromatogr. A 684 (1994) 149.
[27] V. Dolník, M. Deml, P. Boček, J. Chromatogr. 320 (1985) 221.
[28] F. Foret, M. Deml, V. Kahle, P. Boček, Electrophoresis 7 (1986) 430.
[29] J.C. Reijenga, G.V.A. Aben, Th.P.E.M. Verheggen, F.M. Everaerts, J. Chromatogr. 260 (1983) 241.
[30] Th.P.E.M. Verheggen, A.C. Schoots, F.M. Everaerts, J. Chromatogr. 503 (1990) 245.
[31] Th.P.E.M. Verheggen, F.M. Everaerts, J. Chromatogr. 638 (1993) 147.
[32] J.K. Towns, F.E. Regnier, J. Chromatogr. 516 (1990) 69.
[33] T. Hirokawa, M. Nishino, N. Aoki, Y. Kiso, Y. Sawamoto, T. Yagi, J. Akiyama, J. Chromatogr. 271 (1983) D1.
[34] V.A. Palm (Ed.), Tables of Rate and Equilibrium Constants of Heterolytic Organic Reactions, Vol. 2/1, VINITI, Moscow, 1975.
[35] J.L. Becker, F.M. Everaerts, J. Chromatogr. 68 (1972) 207.
[36] P.R. Righetti, M. Pagani, E. Gianazza, J. Chromatogr. 109 (1975) 341.
[37] C. Chiesa, R.A. O'Neill, Electrophoresis 15 (1994) 1132.